MODELLING NOISE-INDUCED FIBRE-ORIENTATION ERROR IN DIFFUSION-TENSOR MRI

Philip A Cook, Daniel C Alexander

Dept. of Computer Science
University College London, UK
p.cook@cs.ucl.ac.uk

Geoffrey J M Parker

Dept. of Imaging Science and Biomedical Engineering
University of Manchester, UK

ABSTRACT

Diffusion-Tensor MRI can be used to measure fibre orientation within the brain. Several studies have proposed methods to reconstruct known white matter fibre tracts in the brain. These methods are known as tractography. However, the measured fibre orientations are subject to error, which leads tractography methods to fail or define false connections. Probabilistic tractography methods use a model of the probability density function (PDF) of the local fibre orientation in each voxel, to calculate the likelihood of any potential fibre pathway through a DT data set. We propose the Watson distribution as a new fibre orientation PDF to replace ad hoc models used previously. We compare the Probabilistic Index of Connectivity (PICo) tractography method using three candidate PDFs and show that the Watson PDF compares favourably to the ad hoc models.

1. INTRODUCTION

Diffusion-weighted magnetic resonance imaging allows *in-vivo* imaging of diffusing water molecule populations as they interact with microscopic cellular structures. Many studies have used the diffusion tensor (DT) [1] to model the statistical properties of diffusing water molecules within the brain. The DT is the 3×3 symmetric covariance matrix of a Gaussian diffusion process in three dimensions, where the probability of a molecule being displaced by a vector $\mathbf{r}$ in time t is

$$p(\mathbf{r}) = \frac{1}{\sqrt{(4\pi t)^3 \det(D)}} \exp\left(-\frac{\mathbf{r}^T D^{-1} \mathbf{r}}{4t}\right). \quad (1)$$

A DT-MRI image is a 3D voxel image where each voxel contains the tensor D that best fits to the diffusion-weighted signals. The voxels typically measure between $5 - 10\text{mm}^3$. The eigen system of D contains three eigenvectors $\mathbf{e}_1$, $\mathbf{e}_2$, $\mathbf{e}_3$, and their corresponding eigenvalues, $\lambda_1 \geq \lambda_2 \geq \lambda_3$. The eigenvalues are proportional to the mean squared displacements along the corresponding eigenvector. The Gaussian distribution has ellipsoidal contours, and DT-MRI is often visualised by plotting an ellipsoidal contour in each voxel, as shown in figure 1.

The trace ($\lambda_1 + \lambda_2 + \lambda_3$) is directly proportional to the mean squared displacement in three dimensions. In free water, the trace is large, and the diffusion is isotropic, so that $\lambda_1 \approx \lambda_2 \approx \lambda_3$. Trace values are much lower in brain tissue, because the cellular structures of the brain tissue restrict the motion of the water molecules. In grey matter (cortical material) the structures restrict the motion more or less equally in all directions (at least at the resolution of DT-MRI) so the diffusion is also isotropic. Within brain white matter (axonal connections), the cellular structures are mostly dense, highly organized bundles of small (about 10^{-6} m in diameter) cylindrical fibres. In white matter, the diffusion is anisotropic, $\lambda_1 \gg \lambda_2 \approx \lambda_3$, because the water has more freedom to move along the fibres than across them. The tensors are elongated in the shape of a cigar, and $\mathbf{e}_1$ should point in the same direction as the fibres in each voxel. We quantify anisotropy using the fractional anisotropy index, which is 0 for a sphere and 1 for an infinitely thin cylinder.

Many groups have studied ways to reconstruct the gross structure of the fibre bundles from DT-MRI data, a study known as "tractography" [2]. A simple method is to propagate a streamline from a starting point, following the local $\mathbf{e}_1$ over a series of small steps. This approach can give a visual impression of the fibre structure, but each streamline is a binary mapping of connectivity; a streamline either connects two points, or it does not. Each voxel measurement is subject to error because of noise, patient motion, and non-Gaussian diffusion behaviour, resulting in erroneous streamline trajectories. Many researchers have imposed heuristic restrictions on streamline behaviour (such as preventing them from bending sharply) in order to cull the most obviously incorrect fibre traces, but again this is a binary mapping (a streamline is accepted as true, or is rejected). Probabilistic methods move beyond the binary

This work was supported by the Medical Images And Signals IRC of the UK Engineering and Physical Sciences Research Council

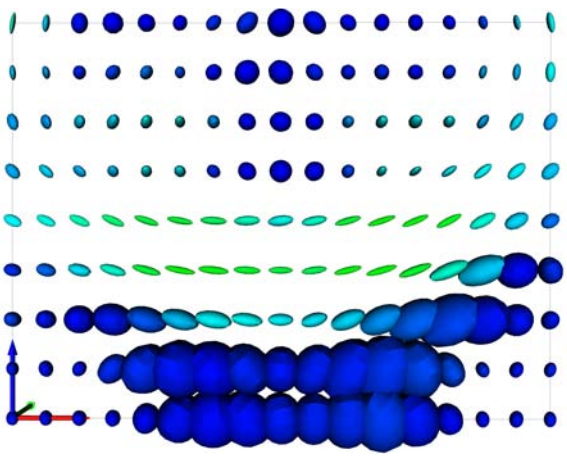

Fig. 1. Ellipsoid contours of tensors showing the curved path of the fibres in the corpus callosum above the fluid-filled ventricles (large ellipsoids).

mapping to define a probability density function (PDF) of any fibre orientation $\mathbf{x}$ in a voxel given D. Given sufficiently accurate fibre-orientation PDFs in each voxel, probabilistic methods allow us to compute the probability of any potential connection within the brain.

2. METHODS

This work introduces a new fibre-orientation PDF using the Watson Distribution on a sphere. The Watson PDF is

$$f(\pm\mathbf{x};\boldsymbol{\mu},\kappa) = M\left(\frac{1}{2},\frac{3}{2},\kappa\right)^{-1}\exp\left[\kappa(\boldsymbol{\mu}^T\mathbf{x})^2\right] \qquad (2)$$

where M denotes the confluent hypergeometric function of the first kind [3, p. 181]. The PDF describes axes, not directions, so $f(\mathbf{e}_1;\boldsymbol{\mu},\kappa) = f(-\mathbf{e}_1;\ \boldsymbol{\mu},\ \kappa)$. This is the behaviour we desire, as the fibre orientation is an axis, without a specified direction.

The parameter κ describes the concentration of the distribution. For $\kappa > 0$, the density has maxima at $\pm\boldsymbol{\mu}$. This is known as the "bipolar distribution". As κ increases, the distribution becomes more concentrated about $\boldsymbol{\mu}$. For $\kappa < 0$, the distribution is concentrated around the great circle orthogonal to $\boldsymbol{\mu}$, this is a "girdle distribution".

When all the fibres within a voxel are straight and parallel, the DT is highly anisotropic, with $\lambda_1 \gg \lambda_2 \approx \lambda_3$, and the best estimate of the fibre orientation is $\mathbf{e}_1$. In this case, the bipolar distribution with $\boldsymbol{\mu} = \mathbf{e}_1$ provides a good model. When two fibres cross within a single voxel, the tensor can become oblate, $\lambda_1 \approx \lambda_2 \gg \lambda_3$, and the ellipsoid is a squashed sphere, like a pancake. The fibre orientations cannot be resolved from the tensor, but the orientations lie close to the plane defined by $\mathbf{e}_1$ and $\mathbf{e}_2$, perpendicular to $\mathbf{e}_3$. In this case the girdle distribution with $\boldsymbol{\mu} = \mathbf{e}_3$ provides a good model.

To determine a suitable value of κ, we find the maximum likelihood estimate of κ using the following theorem from [3]. Assuming that a set of samples comes from a Watson distribution with known $\boldsymbol{\mu}$, we can fit the value of κ numerically. Let $\bar{T}$ be the scatter matrix of n samples $\pm\mathbf{x}_1 \ldots \pm\mathbf{x}_n$, where

$$\bar{T} = \frac{1}{n}\sum_{i=1}^{n}\mathbf{x}_i\mathbf{x}_i^T. \qquad (3)$$

Then the log-likelihood function is

$$\begin{aligned} l &= \kappa\textstyle\sum_{i=1}^{n}(\mathbf{x}_i^T\boldsymbol{\mu})^2 - n\log M\left(\frac{1}{2},\frac{3}{2},\kappa\right) \\ &= n\left[\kappa\boldsymbol{\mu}^T\bar{T}\boldsymbol{\mu} - \log M\left(\frac{1}{2},\frac{3}{2},\kappa\right)\right]. \end{aligned} \qquad (4)$$

Differentiation with respect to κ gives

$$\frac{M\left(\frac{3}{2},\frac{5}{2},\kappa\right)}{3M\left(\frac{1}{2},\frac{3}{2},\kappa\right)} = \hat{\boldsymbol{\mu}}^T\bar{T}\hat{\boldsymbol{\mu}}. \qquad (5)$$

We computed a lookup table that gives us κ as a function of the parameters $\frac{\lambda_1}{\lambda_3}$ and $\frac{\lambda_2}{\lambda_3}$, at a constant trace consistent with white matter ($2100 \times 10^{-6}\text{mm}^2\text{s}^{-1}$) . We generate noise-free synthetic measurements from a tensor with $\mathbf{e}_1$ aligned along the z-axis. We then generate the sample population $\mathbf{x}_i$, $1 \le i \le 10,000$, by adding noise to these synthetic measurements, re-fitting the tensor, and extracting $\mathbf{e}_1$. With $\bar{T}$ and $\boldsymbol{\mu}$ known, we solve equation 5 for κ numerically, using the Newton-Raphson method [4, p. 362]. We solve equation 5 with $\mu = \mathbf{e}_1$ and $\mu = \mathbf{e}_3$, and discard the solution that has the lowest likelihood given the samples.

We tested our PDF within the Probabilistic Index of Connectivity (PICo) [5, 6] framework, which uses Monte-Carlo streamline generation to create maps of connection probability. For each Monte-Carlo iteration, the $\mathbf{e}_1$ of each tensor is aligned with a sample from the voxel PDF, and a streamline is tracked from a manually selected seed point. After N iterations, the probability of connection between the seed point and a point p is $\psi(p)$, which is proportional to the number of streamlines $\chi(p,N)$, that pass through voxel p:

$$\psi(p) = \lim_{N\to\infty}\frac{\chi(p,N)}{N} \approx \frac{\chi(p,N)}{N}. \qquad (6)$$

For cylindrically symmetric tensors, two PDFs for PICo have been demonstrated in brain data [5, 6], both are one-dimensional normal distributions on the angle θ of deflection of $\mathbf{e}_1$. To draw samples from these PDFs, we sample the deflection angle from the normal distribution and rotate about $\mathbf{e}_1$ by an angle drawn from a uniform distribution on $[0, 2\pi]$. The standard deviation σ of the distribution depends

on the anisotropy of the tensor, so that highly anisotropic tensors have the lowest uncertainty. For the PDF used in [5], σ is a sigmoid function of fractional anisotropy, hereafter we will call it the sigmoid PDF. For the PDF used in [6], σ is a biexponential function fitted to the results of numerical simulation of noisy tensors, over a range of anisotropy values. We call this the biexponential PDF. The normal distributions are truncated to give a maximum deflection of 90 degrees.

To test how well each PDF reflected the uncertainty in fibre direction due to noise, we computed PICo maps from each PDF ($N = 10,000$) on synthetic data with simulated noise. As a gold standard, we created a probability map using noise instead of sampling a PDF. For each Monte-Carlo iteration, we added noise to the complex MR signal, and re-fitted the tensor. We then computed the correlation between the map from each PDF and the gold standard.

We use two synthetic data sets: a circular path of radius 20mm, and two perpendicular linear paths that intersect in a region of oblate tensors (see figure 2). We repeat the experiment with tensors over a range of anisotropy values.

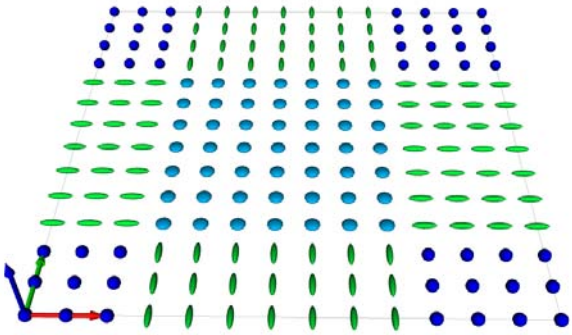

Fig. 2. Synthetic data with fibre crossing.

3. RESULTS AND DISCUSSION

Figure 3 shows the correlation between the gold standard and the PDFs for the circular path data set. We find no significant difference between the Watson PDF and the bi-exponential PDF. The sigmoid PDF produces less focused probability maps, which correlate less well with the ground truth. This PDF was not designed to model only noise, it is a heuristic estimate of total uncertainty caused by effects including noise and the mixing of tissue types within a voxel. Figure 4 shows the difference between the Watson and sigmoid PDF in brain data.

Figure 5 shows the correlation for the crossing fibres. The Watson PDF correlates better than the Gaussian in the case of crossing fibres. For the girdle distribution the PDF is the same around any circle parallel to the plane of $\mathbf{e}_1$ and

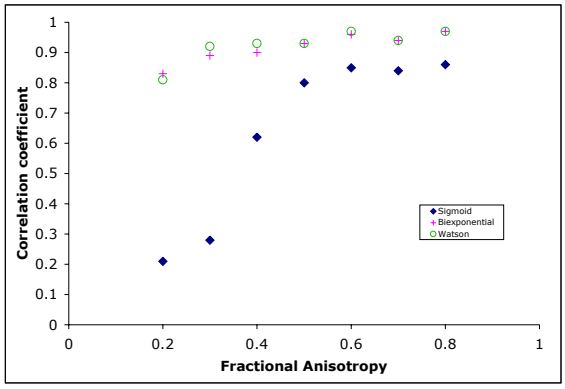

Fig. 3. Correlation of PDF data with gold standard for the circular path.

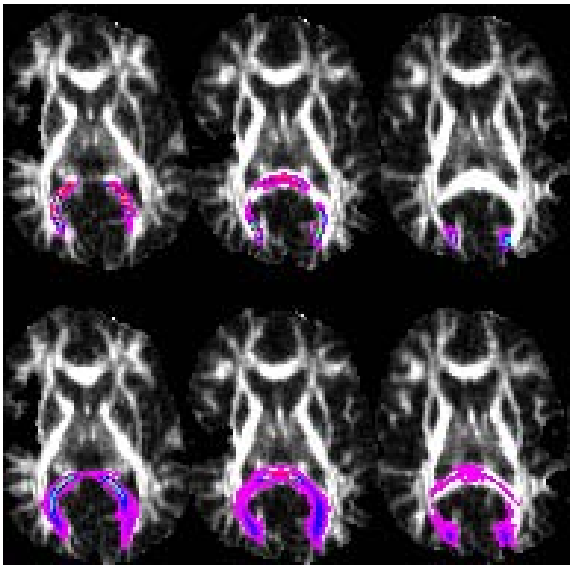

Fig. 4. Three slices from a PICo probability map of connection in splenium of the corpus callosum. The Watson PDF (top) is more concentrated than the sigmoid PDF (bottom).

$\mathbf{e}_2$, so the streamlines spread out within this plane, while the Gaussian PDFs continue to act as the Watson does in the bipolar case, spreading the streamlines in a circularly symmetric cone about $\mathbf{e}_1$. As anisotropy decreases, $\mathbf{e}_3$becomes less trustworthy as a normal to the fibre direction, and the Watson PDF shows increased dispersion in the direction of $\mathbf{e}_3$, until it becomes similar to the Gaussian method.

Both the exponential PDF and the Watson PDF correlate less well to the gold standard at low anisotropy. The estima-

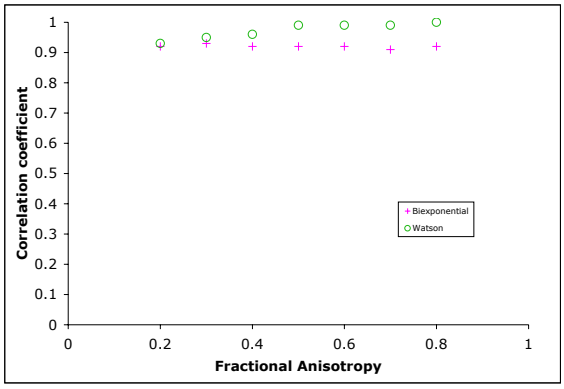

Fig. 5. Correlation of PDF data with gold standard for crossing paths.

tion of κ from equation 5 is sensitive to outliers, and we are currently investigating improvements our lookup table by testing for discordant samples.

While the Watson PDF offers some benefit for dealing with oblate tensors, it is still an unsatisfactory solution for the fibre crossing problem. The uncertainty can be significantly reduced by abandoning the tensor model altogether and using a model that can resolve multiple fibre orientations. Several alternative models have been proposed [7, 8, 9]; once the individual fibre orientations are recovered, the uncertainty could be modelled using any of the PDFs discussed here. This has been shown in [6], where the biexponential PDF is fitted to each of two tensors resolved from voxels that contain crossing fibres The Watson girdle distribution can be used as a fall-back for voxels where the more complex model cannot be fitted satisfactorily. There are also many studies that acquire only enough scanner data to fit the tensor model, and in this case the Watson PDF will be superior to the Gaussian at low concentration, when the truncation of the Gaussian becomes significant, and also in regions of oblate tensors. Furthermore, the Watson model generalises more naturally into a non-cylindrically symmetric axial distribution (the Bingham distribution), which is required in the single-tensor case to model the uncertainty in brain data more accurately.

4. ACKNOWLEDGEMENTS

We would like to thank Olga Ciccarelli and Claudia Wheeler-Kingshott of the Institute of Neurology, University College London, for supplying human brain data.

5. REFERENCES

[1] PJ Basser, J Matiello, and D Le Bihan, "MR diffusion tensor spectroscopy and imaging," *Biophysical Journal*, vol. 66, pp. 259–267, 1994.

[2] Susumu Mori and Peter C. M. van Zijl, "Fiber tracking: principles and strategies: a technical review," *NMR In Biomedicine*, vol. 15, pp. 468–480, 2002.

[3] Kanti V Mardia and Peter E Jupp, *Directional Statistics*, Wiley, 2000.

[4] William H Press, Saul A Teukolsky, William T Vetterling, and Brian P Flannery, *Numerical Recipes in C*, Cambridge University Press, 1992.

[5] Geoffrey J. M. Parker, Claudia A. M. Wheeler-Kingshott, and Hamied A. Haroon, "A framework for a streamline-based probabilistic index of connectivity (pico) using a structural interpretation of mri diffusion measurements," *Journal of Magnetic Resonance Imaging*, vol. 18, pp. 242–254, 2003.

[6] Geoffrey J. M. Parker and Daniel C Alexander, "Probabilistic monte-carlo based mapping of cerebral connections utilising whole-brain crossing fibre information," in *Information Processing in Medical Imaging*, C. J. Taylor and J. A. Noble, Eds. 2003, vol. 2732 of *Lecture Notes in Computer Science*, pp. 684–695, Springer-Verlag.

[7] David S Tuch, *Diffusion MRI of complex tissue structure*, Doctoral dissertation, Harvard-MIT Division of Health Sciences and Technology, 2002.

[8] David S. Tuch, Timothy G. Reese, Mette R. Wiegell, Nikos Makris, John W. Belliveau, and Van J. Wedeen, "High angular resolution diffusion imaging reveals intravoxel white matter fiber heterogeneity," *Magnetic Resonance in Medicine*, vol. 48, pp. 577–582, 2002.

[9] Kalvis M Jansons and Daniel C Alexander, "Persistent angular structure: new insights from diffusion magnetic resonance imaging data," *Inverse Problems*, vol. 19, pp. 1031–1046, 2003.